

Scalable quantum eraser for superconducting integrated circuits

Ciro Micheletti Diniz ^{1,*} Celso J. Villas Bôas ^{1,†} and Alan C. Santos ^{2,‡}

¹*Departamento de Física, Universidade Federal de São Carlos, Rodovia Washington Luís, km 235 - SP-310, 13565-905 São Carlos, SP, Brazil*

²*Instituto de Física Fundamental, Consejo Superior de Investigaciones Científicas, Calle Serrano 113b, 28006 Madrid, Spain*

A fast and scalable scheme for multi-qubit resetting in superconducting quantum processors is proposed by exploiting the feasibility of frequency-tunable transmon qubits and transmon-like couplers to engineer a full programmable superconducting erasing head. The scalability of the device is verified by simultaneously resetting two qubits, where we show that collectivity effects may emerge as an fundamental ingredient to speed up the erasing process. Conversely, we also describe the appearance of decoherence-free subspace in multi-qubit chips, causing it to damage the device performance. To overcome this problem, a special set of parameters for the tunable frequency coupler is proposed, which allows us to erase even states within such subspace. To end, we offer a proposal to buildup integrated superconducting processors that can be efficiently connected to erasure heads in a scalable way.

Introduction.— The pursuit for quantum processing units (QPUs) with long lived qubits resulted in the creation of qubits with coherence time exceeding one hour [1] in single trapped ion-qubit, and few hours with nuclear spins [2]. In state-of-the-art of superconducting quantum computing (QC), the coherence times for transmon qubits ranges from tens [3, 4] to hundreds of microseconds [5], but it may reach a few milliseconds with fluxonium qubits [6]. Besides these achievements constitute a important progress towards the advent of resilient QC, a fundamental operation information processing emerges as a challenge: *the system reinitialization*. As, in general, quantum algorithms need to be repeated thousands or millions of times to achieve fiducial statistical outcomes, fast and scalable approaches for quantum information erasure take place as a fundamental part of the computation.

Due to the impossibility to reset quantum information through coherent unitary operations [7], strategies for efficient reset have been proposed for different species of superconducting QPUs [8–13], with a promising approach [14] exploiting the interaction of the working qubits coupled to quantum-circuit refrigerators [15]. In this way, an external resonator directly coupled to the working qubit will work as an erasure head, responsible for dissipating unknown information encoded in the qubit, with the erasure rate ruled by the resonator decay rate k_r . As a limiting agent in this approach, one cannot speed up the reset by increasing k_r due to the indirect effects of the resonator decay on the qubit lifetime during the QC stage. Therefore, developing scalable and switchable mechanisms to connect qubits to low-quality resonators would be a promising route to engineer faster initialization protocols, since existing approaches address solely individual target qubits resetting [13].

In this letter we describe how to build an erase head able to simultaneously and selectively dissipate quantum information in QPUs with more than one qubit. The device introduced in this letter addresses three fundamental tasks required by any robust erase head: i) Erasing fidelity comparable to fault-tolerance threshold [16]; ii) Resetting times of the order of qubit control time; and iii) Scalability and high controllability. To this end, we use a QPU composed of two qubits connected to a single erase head and we carry out simulations accord-

ing to these distinct fundamental tasks, with special focus on the efficient selective and simultaneous reset. Also, we identify and address collective effects arising in our model (or any other model which includes two or more qubits interacting with an erase head), where a key challenge is to overcome the presence of resilience collective *dark states*, similarly to what is observed for the subradiant states in atomic systems [17–19]. Such states can appear as a direct consequence of the linearity of quantum mechanical systems (superposition principle) and interference phenomena [20], which causes a many-body quantum system prepared in these collective states to be unable to exchange energy with its external environment [21, 22].

The device model.— The model presented in this work is composed of two *working* qubits (used to store and process quantum information) and the full programmable erase head, as sketched in Fig. 1a. The erase head is composed by couplers c_n ($n = 1, 2$), and one qubit q_0 coupled to a dissipative resonator (or waveguide). The working qubits, q_1 and q_2 are *indirectly* connected to the middle qubit q_0 through their respective couplers c_1 and c_2 . Couplers and qubits are considered as two-level systems with lowering $\hat{\sigma}_{c_n}^-$, $\hat{\sigma}_{q_n}^-$, and raising $\hat{\sigma}_{c_n}^+$, $\hat{\sigma}_{q_n}^+$ operators, respectively. The lowering and raising operator for the resonator are \hat{a} and \hat{a}^\dagger , respectively. The device Hamiltonian is given by $\hat{H} = \hat{H}_0 + \hat{H}_{r0} + \hat{H}_{qc}$, with the bare Hamiltonian of the superconducting elements of the circuit (transmons, couplers and resonator) as $H_0 = \sum_n \hbar\omega_{q_n} \hat{\sigma}_{q_n}^+ \hat{\sigma}_{q_n}^- + \sum_n \hbar\omega_{c_n} \hat{\sigma}_{c_n}^+ \hat{\sigma}_{c_n}^- + \hbar\omega_r \hat{a}^\dagger \hat{a}$, with ω_{q_n} , ω_{c_n} and ω_r the natural frequencies of the n -th qubit, n -th coupler and resonator, respectively. The qubit-resonator coupling Hamiltonian given by $\hat{H}_{r0} = g_r \hat{\sigma}_{q_0}^+ \hat{a} + \text{h.c.}$, with interaction strength g_r , and

$$\hat{H}_{qc} = \hbar \sum_{n=1}^2 \left[g_{qc} (\hat{\sigma}_{q_n}^+ + \hat{\sigma}_{q_0}^+) \hat{\sigma}_{c_n}^- + g_p \hat{\sigma}_{q_0}^+ \hat{\sigma}_{q_n}^- + \text{h.c.} \right], \quad (1)$$

describes qubits-couplers and qubit-qubit interactions, with coupling strengths g_{qc} and g_p , respectively. For simplicity, here we assume identical qubit-couplers and qubits-qubits coupling strengths [23]. As we shall see, the switchable performance of the erasing head will be optimal if we build frequency-tunable couplers and qubits (at least the qubit q_0).

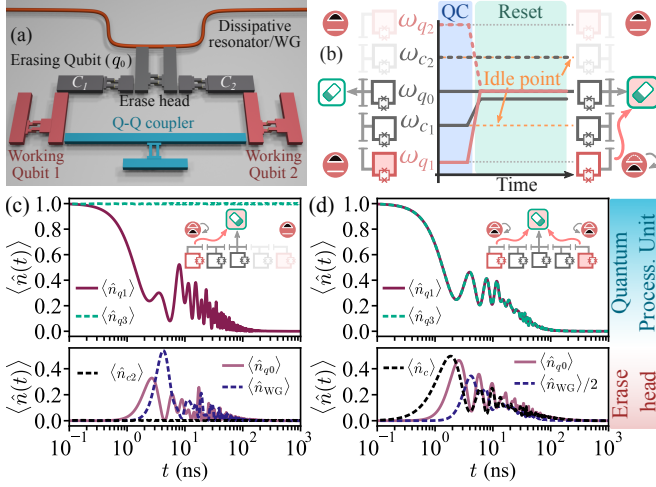


Figure 1. (a) Superconducting device proposed in this work, where two working qubits (1 and 2) interact with the erase head through couplers C_1 and C_2 . A qubit-qubit (Q-Q) coupler is used during the computation stage to perform operations between the working qubits, but it is not used in the erasure stage. (b) The sequence of activation of the erasing head. During the computation stage, the couplers C_1 and C_2 are at their respective idling points. After the computational stage, the frequency of the corresponding coupler of the qubit to be reinitialized is changed to the resonance with the reset frequency, while the other coupler remains at the idling point to protect its qubit to be reset. (c) The population dynamics in the device during the selective process (for q_1), where the top graph show the dynamics population inside the QPU (working qubits), while the bottom graphs show the average excitation number of the cavity mode, qubit q_0 , and the coupler of the non-reset qubit. The parameters for the simultaneous resetting. The panel (d) shows the populations for the simultaneous resetting. The parameters for the device used here are $\omega_{q_n} = \omega_r = 3 \times 2\pi$ GHz, $g_{qc} = g_r = 100 \times 2\pi$ MHz, $g_p = 3 \times 2\pi$ MHz, and $\kappa = 30 \times 2\pi$ MHz. The idle and reset frequencies for the couplers are $\omega_{c_n}^{\text{idle}} \approx 6.3 \times 2\pi$ GHz and $\omega_{c_1} = 3.1 \times 2\pi$ GHz, respectively.

The interaction of strength g_p is the capacitive parasitic qubit-qubit interaction between q_0 and the working qubits, satisfying $|g_p| \ll |g_{qc}|$ [24]. To end, in our model for ideal QPUs, the resetting is done through the dissipative resonator, in such way the system evolves under the local master equation

$$\dot{\hat{\rho}}(t) = \frac{1}{i\hbar} [\hat{H}, \hat{\rho}(t)] + \frac{\kappa}{2} (2\hat{a}\hat{\rho}(t)\hat{a}^\dagger - \{\hat{a}^\dagger\hat{a}, \hat{\rho}(t)\}), \quad (2)$$

where $\hat{\rho}(t)$ is the density matrix of the whole system, and κ is the effective decay rate of the resonator. Through the solution of this equation, the reset fidelity is related to the excitation number of each component of the device, given by $\langle \hat{n}_k \rangle = \text{tr}(\hat{\rho}\hat{n}_k)$, with $\hat{n}_k = \hat{\sigma}_k^+ \hat{\sigma}_k^-$ for two-level systems and $\hat{n}_r = \hat{a}^\dagger \hat{a}$ for the resonator. When $\langle \hat{n}_{q_n} \rangle \approx 0.0$, the n -th qubit is efficiently reset.

Selective and simultaneous resetting.— As an starting point, let us show how to implement the selective and switchable delete of a single qubit in a two-qubit devices. It is done in the dispersive regime of interaction, where the couplers frequency ω_{c_n} satisfy $|\omega_{q_n} - \omega_{c_n}| \gg g_{qc}$, where the effective dynamics is

described by the Hamiltonian [25–27]

$$\hat{H}_{\text{eff}} = (g_{\text{eff}}^{(1)} \hat{\sigma}_{q_1}^+ \hat{\sigma}_{q_0}^- + g_{\text{eff}}^{(2)} \hat{\sigma}_{q_2}^+ \hat{\sigma}_{q_0}^- + g_r \sigma_{q_0}^- \hat{a}^\dagger e^{-i\delta t} + \text{h.c.}), \quad (3)$$

with $\delta = g_{qc}^2 / (\omega_{q_n} - \omega_{c_n})$ and the effective couplings $g_{\text{eff}}^{(n)} = g_p + g_{qc}^2 / \Delta_n$, where we assume all qubits and resonators at frequency $\omega_{q_n} = \omega_r$, but the couplers are detuned from this resonance by $\Delta_n = \omega_r - \omega_{c_n}$. We assume that the selectivity of the resetting can be achieved even when all qubits of the system are in resonance with each other and the erasing head elements. The main consequence of the above result is that $g_{\text{eff}}^{(1)}$ and $g_{\text{eff}}^{(2)}$ are tunable independently through its associated coupler frequency, which allows us to *select* the qubit that will be effectively coupled to the resetting head system. As depicted in Fig. 1b, if we set the frequency of the n -th coupler at its respective idling point frequency $\omega_{c_n}^{\text{idle}}$, that is $\Delta_n^{\text{idle}} = \omega_r - \omega_{c_n}^{\text{idle}} = -g_{qc}^2 / g_p$, we can switch off the coupling of the erasing head with the circuit branch connected to the qubit 1 (if $n = 1$) or qubit 2 (if $n = 2$).

Now, to apply the selective property of our approach, we consider the resetting of the qubit q_1 (similar results are obtained if we choose q_2 instead). In this example, we initialize the system in a state with both working qubits in their respective excited state $|1\rangle$, while rest of the system is in the ground state [28]. As sketched in Fig. 1b, during the QC stage the couplers of the erase head are set at their respective idling points, and therefore the QPU is not affected by the erase head. Then, joint reset of qubits in the QPU can be done by switching on the interaction of the erasing head with the target qubit q_1 , by changing the frequency of the coupler 1 to satisfy $\omega_r - \omega_{c_1}^{\text{res}} \neq \Delta_1^{\text{idle}}$. It leads to an effective triggering of the interaction between the “selected” qubit q_1 and the resetting qubit, and therefore the information stored in q_1 will flow to the resonator through the finite effective interaction with the erasing head, as shown in Fig. 1c.

In a similar way, we can describe how to efficiently use our proposal to simultaneously reset the qubits q_1 and q_2 . To achieve this result, the frequency of both couplers 1 and 2 have to be regulated to satisfy $\omega_r - \omega_{c_n}^{\text{res}} \neq \Delta_n^{\text{idle}}$. By doing this, the information flows simultaneously from the qubits q_1 and q_2 to the resonator through the resetting qubit, as it can be seen from Fig. 1d. This achievement paves the way to a scalable method to reset superconducting circuits, where a single erase head can be used to dissipate the information stored in two (or more) qubits at the same time [25].

Resetting time analysis.— We observed that an unrefined optimization of the resetting time can be done through a simple and suitable choice of the coupling strengths g_{qc} of the couplers with the qubit q_0 , the qubit-resonator coupling g_r , and the resonator dissipation rate κ . Therefore, it is timely to discuss now some conditions to be considered before any approach to compute the optimal resetting time. In fact, the time scales of interest to our device are the decay time of the resonator, given by $\tau_{\text{red}} \sim \kappa^{-1}$, and the exchange time between the qubit q_2 and the resonator, given by $\tau_{\text{exc}} \sim |g_r|^{-1}$. In this part of the device, it is important to avoid a coherent back-

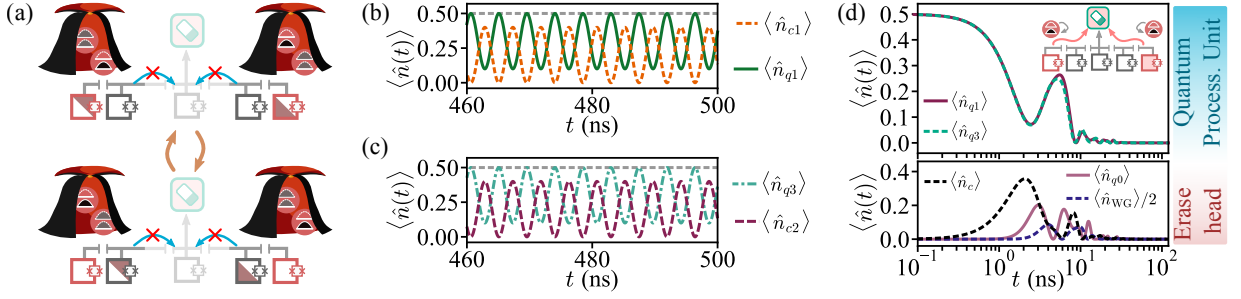


Figure 2. (a) Sketch of the dark state dynamics of the system which inhibits the qubit reset, as the information gets trapped in the system constituted by the working qubits and their respective couplers. (b) Population dynamics for the system $q_1 - c_1$ and (c) $q_2 - c_2$ as function of the time. Gray dashed lines in (b) and (c) represents the total population in the system $q_1 - c_1$ and $q_2 - c_2$, respectively. (d) Population dynamics in the working qubits (top) and erasing head components showing the simultaneous reset of a dark state. We set $g_r = 120 \times 2\pi$ MHz and $\kappa = 150 \times 2\pi$ MHz, and the other parameters are as stated in Fig. 1.

flow of information from the resonator to the qubit q_2 , leading the system dynamics to a non-Markovian regime which will negatively affect the resetting performance of the device. For example, such a coherent backflow can be observed in Figs. 1c-d through the oscillations of the qubits and resonator populations. Therefore, a first condition to be considered is the weak coupling regime of q_0 and resonator, expressed by the relation $|g_r| < \kappa$. We also can state the additional condition $g_{qc} < g_r$ for the couplings strengths, in order to mitigate information backflow from the qubit q_0 to the coupler c_1 . Likewise, when considering the resetting of qubit q_2 , this last condition also helps to avoid the information backflow from the qubit q_0 to the coupler c_2 . From this preliminary discussion, enhancement in the resetting time is expected when $g_{qc} < g_r < \kappa$. This optimization strategy will be used soon, by dealing with the efficient reset of classes of states resilient against deletion.

Here, the question of interest is: How fast the simultaneous reset of two qubits can be in comparison with respect to the single-qubit reset performance? To address this point, one defines the *resetting time*, τ_{res} , as the minimum time spent to delete the information with fidelity above a threshold \mathcal{F}_{tsh} . It is desirable that $\mathcal{F}_{\text{tsh}} = 99.5\%$, a fidelity comparable to two-qubit gate fidelity required for high performance near-term devices [16]. From the data shown in Fig. 1, we determine the resetting time for single qubit selective reset as $\tau_{\text{res}}^{\text{sq}} \approx 296.3$ ns. We computed the time $\tau_{\text{res}}^{\text{sim}}$ required for simultaneous reset of the qubits q_1 and q_2 we found the relation $\tau_{\text{res}}^{\text{sim}} \approx 0.77\tau_{\text{res}}^{\text{sq}}$, that is, simultaneous resetting of two qubits is slightly faster than the single qubit case. This can be explained through the emergence of cooperative behavior in the system along the evolution, as we shall discuss now.

Collective effects.— Now we will show how many-body collectivity may affect the device performance, in which we will pay special attention to overlooked problem of quantum resetting devices: the emergence of collective dark states. To this end, let us consider the simultaneous resetting with all system at resonance, such that the driving Hamiltonian can be written (in the interaction picture) as $\hat{H}_I = \hat{H}_{qc}$. Now, consider the task of delete the two-qubit states of the form

$|\psi_\phi\rangle_{q_1q_2} \propto |10\rangle_{q_1q_2} + e^{i\phi}|01\rangle_{q_1q_2}$, for an arbitrary phase $\phi \in \mathbb{R}$. To this particular state, it is possible to show that for the initial state $|\Psi_\phi\rangle = |\psi_\phi\rangle_{q_1q_2} |000\rangle_{q_0c_1c_2}$ we get

$$\hat{H}_{qc} |\Psi_\phi\rangle \propto g_{qc} |\psi_\phi\rangle_{c_1c_2} |000\rangle_{q_0,1,2} + \frac{(1 + e^{i\phi})g_p}{\sqrt{2}} |1\rangle_{q_0} |0000\rangle_{q_1,2c_1,2}, \quad (4)$$

where the first term describes the initial transfer rate of information from QPU to the couplers, and the second term is the transfer rate from the QPU to the qubit q_0 . As a first remark, consider the case in which $\phi = 2n\pi$, $n \in \mathbb{Z}$, where the coefficient of the second term becomes $\sqrt{2}g_p$. This result suggests a super-radiant enhancement in the coupling between the qubits and the erasing head through the parasitic interaction. As a first conclusion, parasitic and collateral interactions may enhance the simultaneous resetting time of entangled states $|\psi_{\phi=2n\pi}\rangle$. This result explains why the simultaneous reset is faster than the single qubit case, as the information flows from the QPU to the couplers while populating the super-radiant state $|\psi_\phi\rangle_{c_1c_2}$ for the couplers, as shown in Eq. (4). This result also explain the collective enhancements of resetting Dicke states for an arbitrary number of qubits N [29]. In fact, we observe that such a super-radiant coupling enhancement proportional to the number of qubits N may lead to an effective decreasing of the resetting time of our device.

Now, let us focus on the state with $\phi = (2n + 1)\pi$, $n \in \mathbb{Z}$, where any transfer rate to the state $|1\rangle_{q_0} |0000\rangle_{q_1,2c_1,2}$ in Eq. (4) vanishes, leading to a perfectly dark state of the QPU with respect to the qubit q_0 . Moreover, it is possible to show that [25]

$$\hat{H}_{qc}^2 |\Psi_{\phi=(2n+1)\pi}\rangle \propto \hbar^2 g_{qc}^2 |\Psi_{\phi=(2n+1)\pi}\rangle, \quad (5)$$

due to destructive superposition of terms $\hat{\sigma}_{q_0}^+ \hat{\sigma}_{c_1}^- |\psi_\phi\rangle_{c_1c_2} |000\rangle_{q_0,1,2}$ and $\hat{\sigma}_{q_0}^+ \hat{\sigma}_{c_2}^- |\psi_\phi\rangle_{c_1c_2} |000\rangle_{q_0,1,2}$. From this analysis one concludes that, as illustrated in Fig. 2a, the state $|\psi_{\text{dark}}(0)\rangle = |\Psi_{\phi=(2n+1)\pi}\rangle$ cannot be reset because no excitation is transferred to the resetting head, creating then a QPU- q_0 dark state. According to this result, in this case the excitation is “trapped” in the system composed by the couplers and working qubits. In Fig. 2b, the evolution of

the system shows this finding in a more concise way, which corroborates to the result suggested by the Fig. 2a, showing the coherent population exchange between the working qubits and their respective couplers, while the population in qubit q_0 remains zero during the evolution (as the initial excitation remains “trapped” in the systems $q_1 - c_1$ and $q_2 - c_2$). The existence of such dark states, as shown above, should also be observed in other resetting models, like the ones proposed in Refs. [29, 30], given the collective nature of the interactions [25].

In this regard, the development of strategies to deal with such dark states in any physical resetting device is a key task we have to pay attention. In our model, in particular, we show below a robust way to avoid any residual amount of information stored in dark states for any initial state of the working qubits $|\psi(0)\rangle$. One possible, and efficient, solution can be achieved through engineering time-dependent Hamiltonians. In fact, in this way, given a dark state for the Hamiltonian at a given time $t = 0$, such a state is affected (deleted) if it is not dark state of the Hamiltonian at a time $t > 0$. Also, in order to implement the protocol as faster and controllable as we can, it is desired that such a time-dependence can appear naturally during the evolution. In other words, without the requirement of any time-dependent external parameter. Now, we show how this can be achieved in our device by properly adjusting the couplers frequency.

First of all, let's write the Hamiltonian \hat{H}_{qc} in the interaction picture as (with $\Delta_{c_n} = \omega_r - \omega_{c_n}$)

$$H_I(t) = \hbar \sum_{n=1}^2 \left[g_{qc} (\hat{\sigma}_{q_n}^+ + \hat{\sigma}_{q_0}^+) \hat{\sigma}_{c_n}^- e^{i\Delta_{c_n}t} + g_p \hat{\sigma}_{q_n}^+ \hat{\sigma}_{q_0}^- + \text{h.c.} \right], \quad (6)$$

where we assumed that all qubits and resonator are at resonance frequency ω_r , but the couplers are in different frequencies. Then, the key ingredients in our analysis are the time-dependent phases appearing in the first term of the Hamiltonian $H_I(t)$. In this way, it is possible to see that when $\Delta_{c_1} \neq \Delta_{c_2}$ the state $|\Psi_{\phi=(2n+1)\pi}\rangle$ is a dark state for the Hamiltonian only at a given time $t = 0$, but it may be affected (deleted) because it is a bright state of the evolved Hamiltonian for $t > 0$.

As showed in Fig. 2c, we are able to reset the state $|\Psi_{\phi=(2n+1)\pi}\rangle$ imposing the condition $\omega_{c_1} \neq \omega_{c_2}$, where these frequencies are adjusted to complete the resetting in $\tau_{\text{res}}^{\text{sim}} \approx 27$ ns. It is worth to highlight here that the suitable choice of values for this case allows us to speed up the resetting procedure in comparison with Fig. 1, even when we deal with initial resilient states. The frequencies ω_{c_n} that allow the resetting of possible dark states and yield fast erasing depend on the coupling strengths and qubits frequencies. Because of that, such frequencies ω_{c_n} may have different relationship, according to the specifications of each device. This strategy can be reached, for instance, by properly adjusting the frequencies of the couplers through external flux lines [31, 32], paving the way to the scalability feature of our device.

Device scalability.— In this section we study the scalability aspect of our proposal. In Fig. 3 we present a pictorial way

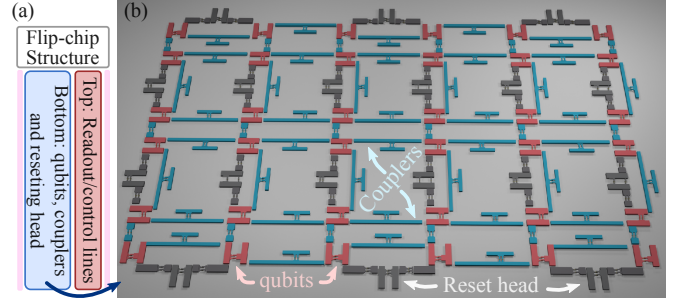


Figure 3. (a) Flip-chip structure of a (b) scalable QPU, with erasing heads dedicated to delete independent cells of two-qubits.

on how to engineer a superconducting integrated circuit with dedicated erasing heads. One possible technology required for such a device can be found from techniques to build 3D flip-chip integrated superconducting circuits [33], as depicted in Fig. 3a. Through flip-chip approach, each plate of the chip can be fabricated separately, in such way the device consists of one *processing chip*, where one deposits the qubits used for information processing, and one *control chip*, where all machinery needed to control/read quantum information is placed at. Here we propose the integration of the dedicated erasing heads in the *processing chip*, in such way that the controllability of the selective and simultaneous reset can be done through additional control lines in the *control chip*. Our proposal is supported by the advantages of using flip-chip processors reported in literature, with respect to single-chip in planar circuits. For example, the methods for fabrication of integrated superconducting circuits developed in Ref. [33] allowed for a reduced degradation of the qubits performance when compared with single-chip devices, leading to enhanced gate fidelities and coherence times exceeding 90 μs (in average). These values of coherence in 3D integrated circuits can be even longer, as those ones reported in Ref. [34], where energy relaxation times around 149 μs have been reached in a device with out-of-plane control lines [35], in a similar way as sketched in Fig. 3a. In addition to these two examples, many other progresses have been done in this direction over the past couple of years [36–41].

By harnessing the current state-of-the-art aforementioned, we propose the $N \times M$ (for arbitrary N and M) topology of quantum chip. As an example, in Fig. 3b we show a 6×6 lattice with pairwise dedicated erasing heads. The coupling between the qubits are engineered through frequency tunable couplers directly connecting the two adjacent qubits, while the reset system connects such qubits in a similar way. Through this design, the selective property of our device allows us to reinitialize any arbitrary portion of the system in a controlled way.

Conclusions.— In this work we proposed a superconducting quantum eraser for fast and high-fidelity quantum information reset. The engineered device is built with focus on its feasibility and tunability, demonstrated through the selective reset of a given qubit in a multi-qubit processor. The scalability

of the model is investigated by successfully performing the collective restart of multi-qubits devices, where we showed how the collective effects (super-radiance) may enhance the device effectiveness. In this context, in advance we identified the emergence of resilient states due to the intrinsic collective effects when quantum eraser is coupled to more than one qubit simultaneously. However, we showed how the proposed device can efficiently face with the emergence of these resilient states through a suitable change of tunable parameters of the system. To end, we proposed an experimentally feasible sketch of a quantum processor composed of working qubits and qubit-qubit tunable couplers integrated with two-qubit dedicated quantum erasers. Such a scheme can be adapted to consider three-qubit dedicated erasing heads.

Our work shades light on the emergence of collective phenomena as a fundamental problem for quantum information resetting, and paves the way for further developments of superconducting processors integrated to scalable and robust quantum erasers.

C.M.D. is supported by the São Paulo Research Foundation (FAPESP, Grant No. 2022/10218-2). C.J.V.-B. acknowledges the supported by the Sao Paulo Research Foundation (FAPESP, Grant No. 2022/00209-6) and by the Brazilian National Council for Scientific and Technological Development (CNPq, Grant 311612/2021-0). A.C.S. acknowledges the support by the European Union's Horizon 2020 FET-Open project SuperQuLAN (899354) and Comunidad de Madrid Sinérgicos 2020 project NanoQuCo-CM (Y2020/TCS-6545).

* ciromd@outlook.com.br

† celsovb@df.ufscar.br

‡ ac_santos@iff.csic.es

- [1] P. Wang, C.-Y. Luan, M. Qiao, M. Um, J. Zhang, Y. Wang, X. Yuan, M. Gu, J. Zhang, and K. Kim, *Nature communications* **12**, 233 (2021).
- [2] M. Zhong, M. P. Hedges, R. L. Ahlefeldt, J. G. Bartholomew, S. E. Beavan, S. M. Wittig, J. J. Longdell, and M. J. Sellars, *Nature* **517**, 177 (2015).
- [3] J. Chu, X. He, Y. Zhou, J. Yuan, L. Zhang, Q. Guo, Y. Hai, Z. Han, C.-K. Hu, W. Huang, H. Jia, D. Jiao, Y. Liu, Z. Ni, X. Pan, J. Qiu, W. Wei, Z. Yang, J. Zhang, Z. Zhang, W. Zou, Y. Chen, X. Deng, X. Deng, L. Hu, J. Li, D. Tan, Y. Xu, T. Yan, X. Sun, F. Yan, and D. Yu, *Nature Physics* **19**, 126 (2022).
- [4] Z. Han, C. Lyu, Y. Zhou, J. Yuan, J. Chu, W. Nuerbolati, H. Jia, L. Nie, W. Wei, Z. Yang, L. Zhang, Z. Zhang, C.-K. Hu, L. Hu, J. Li, D. Tan, A. Bayat, S. Liu, F. Yan, and D. Yu, *Phys. Rev. Res.* **6**, 013015 (2024).
- [5] A. P. M. Place, L. V. H. Rodgers, P. Mundada, B. M. Smitham, M. Fitzpatrick, Z. Leng, A. Premkumar, J. Bryon, A. Vrajitoarea, S. Sussman, G. Cheng, T. Madhavan, H. K. Babla, X. H. Le, Y. Gang, B. Jäck, A. Gyenis, N. Yao, R. J. Cava, N. P. de Leon, and A. A. Houck, *Nature Communications* **12**, 1779 (2021).
- [6] A. Somoroff, Q. Ficheux, R. A. Mencia, H. Xiong, R. Kuzmin, and V. E. Manucharyan, *Phys. Rev. Lett.* **130**, 267001 (2023).
- [7] A. Kumar Pati and S. L. Braunstein, *Nature* **404**, 164 (2000).
- [8] P. Magnard, P. Kurpiers, B. Royer, T. Walter, J.-C. Besse, S. Gasparinetti, M. Pechal, J. Heinsoo, S. Storz, A. Blais, and A. Wallraff, *Phys. Rev. Lett.* **121**, 060502 (2018).
- [9] M. D. Reed, B. R. Johnson, A. A. Houck, L. DiCarlo, J. M. Chow, D. I. Schuster, L. Frunzio, and R. J. Schoelkopf, *Applied Physics Letters* **96**, 203110 (2010).
- [10] K. Geerlings, Z. Leghtas, I. M. Pop, S. Shankar, L. Frunzio, R. J. Schoelkopf, M. Mirrahimi, and M. H. Devoret, *Phys. Rev. Lett.* **110**, 120501 (2013).
- [11] D. Egger, M. Werninghaus, M. Ganzhorn, G. Salis, A. Fuhrer, P. Müller, and S. Filipp, *Phys. Rev. Appl.* **10**, 044030 (2018).
- [12] Y. Sunada, S. Kono, J. Ilves, S. Tamate, T. Sugiyama, Y. Tabuchi, and Y. Nakamura, *Phys. Rev. Appl.* **17**, 044016 (2022).
- [13] C. M. Diniz, R. J. de Assis, N. G. de Almeida, and C. J. Villas-Boas, *Phys. Rev. A* **108**, 052605 (2023).
- [14] T. Yoshioka, H. Mukai, A. Tomonaga, S. Takada, Y. Okazaki, N.-H. Kaneko, S. Nakamura, and J.-S. Tsai, *Phys. Rev. Appl.* **20**, 044077 (2023).
- [15] K. Y. Tan, M. Partanen, R. E. Lake, J. Govenius, S. Masuda, and M. Möttönen, *Nature Communications* **8**, 15189 (2017).
- [16] S. Boixo, S. V. Isakov, V. N. Smelyanskiy, R. Babbush, N. Ding, Z. Jiang, M. J. Bremner, J. M. Martinis, and H. Neven, *Nature Physics* **14**, 595 (2018).
- [17] M. Gegg, A. Carmele, A. Knorr, and M. Richter, *New Journal of Physics* **20**, 013006 (2018).
- [18] A. Albrecht, L. Henriot, A. Asenjo-Garcia, P. B. Dieterle, O. Painter, and D. E. Chang, *New Journal of Physics* **21**, 025003 (2019).
- [19] H. Cheng and W. Nie, *Communications in Theoretical Physics* **76**, 085101 (2024).
- [20] C. J. Villas-Boas, C. E. Máximo, P. P. de Souza, R. Bachelard, and G. Rempe, “Bright and dark states of light: The quantum origin of classical interference,” (2024), [arXiv:2112.05512 \[quant-ph\]](https://arxiv.org/abs/2112.05512).
- [21] P. M. Alsing, D. A. Cardimona, and H. J. Carmichael, *Phys. Rev. A* **45**, 1793 (1992).
- [22] O. Rubies-Bigorda and S. F. Yelin, *Phys. Rev. A* **106**, 053717 (2022).
- [23] The theory is developed consider a chirality of the device with respect to the central qubit q_0 , but the main results obtained here are achievable through non-chiral devices.
- [24] P. Rosario, A. C. Santos, C. Villas-Boas, and R. Bachelard, *Phys. Rev. Appl.* **20**, 034036 (2023).
- [25] See Supplemental Material at [URL will be inserted by publisher] for further details on the derivation of the effective Hamiltonian of the system of qubits considered in this work, simulations for three and four working qubits is also presented to exemplify the scalable aspect of our method, and a discussion on the emergence of dark state in other proposals of multi-qubit resetting, and a list of additional references which also include the Refs [29, 30].
- [26] D. James, *Fortschritte der Physik* **48**, 823 (2000).
- [27] D. F. James and J. Jerke, *Canadian Journal of Physics* **85**, 625 (2007), <https://doi.org/10.1139/p07-060>.
- [28] Without loss of generality we can study the operation of the system taking the excited state $|1\rangle$ as reference for reset, once for any state of the form $|\psi\rangle = a|0\rangle + b|1\rangle$, only the component $|1\rangle$ will be affected by the resetting task.
- [29] Y. Liu, C. Huang, X. Zhang, and D. He, “Collective advantages in qubit reset: effect of coherent qubits,” (2024), [arXiv:2407.03096 \[quant-ph\]](https://arxiv.org/abs/2407.03096).
- [30] T. Li, K. W. Chan, K. Y. Tan, J. Goetz, and M. Möttönen, *World Intellectual Property Organization (WIPO No. EP3933716A1)*

- (2022).
- [31] Z. Ni, S. Li, L. Zhang, J. Chu, J. Niu, T. Yan, X. Deng, L. Hu, J. Li, Y. Zhong, S. Liu, F. Yan, Y. Xu, and D. Yu, *Phys. Rev. Lett.* **129**, 040502 (2022).
- [32] C.-K. Hu, J. Yuan, B. A. Veloso, J. Qiu, Y. Zhou, L. Zhang, J. Chu, O. Nurbolat, L. Hu, J. Li, Y. Xu, Y. Zhong, S. Liu, F. Yan, D. Tan, R. Bachelard, A. C. Santos, C. Villas-Boas, and D. Yu, *Phys. Rev. Appl.* **20**, 034072 (2023).
- [33] S. Kosen, H.-X. Li, M. Rommel, D. Shiri, C. Warren, L. Grönberg, J. Salonen, T. Abad, J. Biznárová, M. Caputo, L. Chen, K. Grigoras, G. Johansson, A. F. Kockum, C. Križan, D. P. Lozano, G. J. Norris, A. Osman, J. Fernández-Pendás, A. Ronzani, A. F. Roudsari, S. Simbierowicz, G. Tancredi, A. Wallraff, C. Eichler, J. Govenius, and J. Bylander, *Quantum Science and Technology* **7**, 035018 (2022).
- [34] P. A. Spring, S. Cao, T. Tsunoda, G. Campanaro, S. Fasciati, J. Wills, M. Bakr, V. Chidambaram, B. Shteynas, L. Carpenter, P. Gow, J. Gates, B. Vlastakis, and P. J. Leek, *Science Advances* **8**, eabl6698 (2022).
- [35] J. Rahamim, T. Behrle, M. J. Peterer, A. Patterson, P. A. Spring, T. Tsunoda, R. Manenti, G. Tancredi, and P. J. Leek, *Applied Physics Letters* **110**, 222602 (2017).
- [36] D. Rosenberg, D. Kim, R. Das, D. Yost, S. Gustavsson, D. Hover, P. Krantz, A. Melville, L. Racz, G. O. Samach, S. J. Weber, F. Yan, J. L. Yoder, A. J. Kerman, and W. D. Oliver, *npj Quantum Information* **3**, 42 (2017).
- [37] A. Patterson, J. Rahamim, T. Tsunoda, P. Spring, S. Jebari, K. Ratter, M. Mergenthaler, G. Tancredi, B. Vlastakis, M. Esposito, and P. Leek, *Phys. Rev. Appl.* **12**, 064013 (2019).
- [38] Y. Wu, W.-S. Bao, S. Cao, F. Chen, M.-C. Chen, X. Chen, T.-H. Chung, H. Deng, Y. Du, D. Fan, M. Gong, C. Guo, C. Guo, S. Guo, L. Han, L. Hong, H.-L. Huang, Y.-H. Huo, L. Li, N. Li, S. Li, Y. Li, F. Liang, C. Lin, J. Lin, H. Qian, D. Qiao, H. Rong, H. Su, L. Sun, L. Wang, S. Wang, D. Wu, Y. Xu, K. Yan, W. Yang, Y. Yang, Y. Ye, J. Yin, C. Ying, J. Yu, C. Zha, C. Zhang, H. Zhang, K. Zhang, Y. Zhang, H. Zhao, Y. Zhao, L. Zhou, Q. Zhu, C.-Y. Lu, C.-Z. Peng, X. Zhu, and J.-W. Pan, *Phys. Rev. Lett.* **127**, 180501 (2021).
- [39] X. Li, Y. Zhang, C. Yang, Z. Li, J. Wang, T. Su, M. Chen, Y. Li, C. Li, Z. Mi, X. Liang, C. Wang, Z. Yang, Y. Feng, K. Linghu, H. Xu, J. Han, W. Liu, P. Zhao, T. Ma, R. Wang, J. Zhang, Y. Song, P. Liu, Z. Wang, Z. Yang, G. Xue, Y. Jin, and H. Yu, *Applied Physics Letters* **119**, 184003 (2021).
- [40] C. R. Conner, A. Bienfait, H.-S. Chang, M.-H. Chou, É. Dumur, J. Grebel, G. A. Peairs, R. G. Povey, H. Yan, Y. P. Zhong, and A. N. Cleland, *Applied Physics Letters* **118**, 232602 (2021).
- [41] A. Gold, J. P. Paquette, A. Stockklauser, M. J. Reagor, M. S. Alam, A. Bestwick, N. Didier, A. Nersisyan, F. Oruc, A. Razavi, B. Scharmann, E. A. Sete, B. Sur, D. Venturelli, C. J. Winkleblack, F. Wudarski, M. Harburn, and C. Rigetti, *npj Quantum Information* **7**, 142 (2021).

Supplemental Material for: Scalable quantum eraser for superconducting integrated circuits

Ciro Micheletti Diniz ^{1,*} C. J. Villas-Boas ^{1,†} and Alan C. Santos ^{2,‡}

¹*Departamento de Física, Universidade Federal de São Carlos, Rodovia Washington Luís, 13565-905 São Carlos, SP, Brazil*

²*Instituto de Física Fundamental, Consejo Superior de Investigaciones Científicas, Calle Serrano 113b, 28006 Madrid, Spain*

*ciromd@outlook.com.br, †celsovb@df.ufscar.br, ‡ac_santos@df.ufscar.br

Effective Hamiltonian and robustness against dark states effects

The device Hamiltonian is given by $\hat{H} = \hat{H}_0 + \hat{H}_{r0} + \hat{H}_{qc}$. The bare Hamiltonian of the superconducting elements of the circuit (transmons, couplers and resonator) reads $\hat{H}_0 = \sum_{i=0}^2 \hbar \omega_{q_i} \hat{\sigma}_{q_i}^+ \hat{\sigma}_{q_i}^- + \sum_{j=1}^2 \hbar \omega_{c_j} \hat{\sigma}_{c_j}^+ \hat{\sigma}_{c_j}^- + \hbar \omega_r \hat{a}^\dagger \hat{a}$, where ω_X is the transition frequency of the component X , which can be the qubits q_i , the couplers c_j , or the cavity mode. The erase head qubit-resonator coupling Hamiltonian is $\hat{H}_{r0} = g_r \hat{\sigma}_{q_0}^+ \hat{a} + \text{h.c.}$, where g_r is the respective coupling strength. Also, the Hamiltonian that describes the qubit-coupler and qubit-qubit interactions is given by

$$\hat{H}_{qc} = \hbar \sum_{n=1}^2 \left[g_{qc} (\hat{\sigma}_{q_n}^+ + \hat{\sigma}_{q_0}^+) \hat{\sigma}_{c_n}^- + g_p \hat{\sigma}_{q_0}^+ \hat{\sigma}_{q_n}^- + \text{h.c.} \right], \quad (\text{S1})$$

where we assume identical qubit-coupler and qubit-qubit coupling strengths, respectively, denoted by g_{qc} and g_p . The following derivation considers a chiral device with respect to the central qubit q_0 , but the deduction for non-chiral devices is similar.

We start moving to the interaction picture by applying the unitary transformation $\hat{U}_0(t) = \exp(-i\hat{H}_0 t)$, with \hat{H}_0 defined above, considering the qubits and the resonator in resonance with frequency $\omega_{q_n} = \omega_r$ (this assumption is particularly true during the resetting task). Hence, we obtain the Hamiltonian $\hat{H}^{(I)} = \hat{U}_0^\dagger(t) \hat{H} \hat{U}_0(t) - \hat{H}_0$ that reads

$$\hat{H}^{(I)} = g_{qc} (\hat{\sigma}_{q_1}^+ + \hat{\sigma}_{q_0}^+) \hat{\sigma}_{c_1}^- e^{i\Delta_1 t} + g_{qc} (\hat{\sigma}_{q_0}^+ + \hat{\sigma}_{q_2}^+) \hat{\sigma}_{c_2}^- e^{i\Delta_2 t} + g_p \hat{\sigma}_{q_1}^+ \hat{\sigma}_{q_0}^- + g_p \hat{\sigma}_{q_0}^+ \hat{\sigma}_{q_2}^- + g_r \hat{\sigma}_{q_0}^+ \hat{a} + \text{h.c.},$$

where $\Delta_1 = \omega_r - \omega_{c_1}$, and $\Delta_2 = \omega_r - \omega_{c_2}$. For detunings Δ_1 and Δ_2 much higher than the coupling g_{qc} , we can derive an effective Hamiltonian via [26, 27]

$$\hat{H}_{\text{eff}}^{(I)} = -i\hat{H}^{(I)}(t) \int_0^t \hat{H}^{(I)}(t') dt'. \quad (\text{S2})$$

Then, by applying the rotating wave approximation (RWA) and by assuming that the couplers C_1 and C_2 remain in their respective ground states during the dispersive interaction, we obtain the effective Hamiltonian

$$\begin{aligned} \hat{H}_{\text{eff}}^{(I)} &= \frac{g_{qc}^2}{\Delta_1} \hat{\sigma}_{q_1}^+ \hat{\sigma}_{q_1}^- + \left(\frac{g_{qc}^2}{\Delta_1} + \frac{g_{qc}^2}{\Delta_2} \right) \hat{\sigma}_{q_0}^+ \hat{\sigma}_{q_0}^- + \left(\frac{g_{qc} g_{qc}}{\Delta_1} + g_p \right) (\hat{\sigma}_{q_1}^+ \hat{\sigma}_{q_0}^- + \text{h.c.}) + \left(\frac{g_{qc} g_{qc}}{\Delta_2} + g_p \right) (\hat{\sigma}_{q_2}^+ \hat{\sigma}_{q_0}^- + \text{h.c.}) \\ &+ \frac{g_{qc}^2}{\Delta_2} \hat{\sigma}_{q_2}^+ \hat{\sigma}_{q_2}^- + g_r (\hat{\sigma}_{q_0}^+ \hat{a} + \hat{\sigma}_{q_0}^- \hat{a}^\dagger). \end{aligned} \quad (\text{S3})$$

Moving back to the Schrödinger picture using the unitary transformation $\hat{H}_{\text{eff}}^{(\text{SC})} = \hat{U}_0(t) \hat{H} \hat{U}_0^\dagger(t) + \hat{H}_0$, we obtain the full effective Hamiltonian

$$\begin{aligned} \hat{H}_{\text{eff}}^{(\text{SC})} &= \sum_{i=0}^2 \Omega_{q_i} \hat{\sigma}_{q_i}^+ \hat{\sigma}_{q_i}^- + \sum_{j=1}^2 \omega_{c_j} \hat{\sigma}_{c_j}^+ \hat{\sigma}_{c_j}^- + \left(\frac{g_{qc} g_{qc}}{\Delta_1} + g_p \right) (\hat{\sigma}_{q_1}^+ \hat{\sigma}_{q_0}^- + \text{h.c.}) \\ &+ \left(\frac{g_{qc} g_{qc}}{\Delta_2} + g_p \right) (\hat{\sigma}_{q_2}^+ \hat{\sigma}_{q_0}^- + \text{h.c.}) + g_r (\hat{\sigma}_{q_0}^+ \hat{a} + \hat{\sigma}_{q_0}^- \hat{a}^\dagger) + \omega_r \hat{a}^\dagger \hat{a}, \end{aligned} \quad (\text{S4})$$

where $\Omega_{q_1} = \omega_r + \frac{g_{qc}^2}{\Delta_1}$, $\Omega_{q_0} = \omega_r + \frac{g_{qc}^2}{\Delta_1} + \frac{g_{qc}^2}{\Delta_2}$, and $\Omega_{q_2} = \omega_r + \frac{g_{qc}^2}{\Delta_2}$. Thus, from Eq. (S4) we can derive the effective interaction Hamiltonian in the interaction picture as

$$\hat{H}_{\text{eff}} = \left(\frac{g_{qc} g_{qc}}{\Delta_1} + g_p \right) \hat{\sigma}_{q_1}^+ \hat{\sigma}_{q_0}^- e^{i(\Omega_1 - \Omega_0)t} + \left(\frac{g_{qc} g_{qc}}{\Delta_2} + g_p \right) \hat{\sigma}_{q_2}^+ \hat{\sigma}_{q_0}^- e^{i(\Omega_2 - \Omega_0)t} + g_r \hat{\sigma}_{q_0}^- \hat{a}^\dagger e^{i(\omega_r - \Omega_0)t} + \text{h.c.}, \quad (\text{S5})$$

which can be rewritten as (up to a global phase)

$$\hat{H}_{\text{eff}} = g_{\text{eff}}^{(1)} \hat{\sigma}_{q_1}^+ \hat{\sigma}_{q_0}^- e^{i \frac{g_{\text{qc}}^2}{\Delta_1} t} + g_{\text{eff}}^{(2)} \hat{\sigma}_{q_2}^+ \hat{\sigma}_{q_0}^- e^{i \frac{g_{\text{qc}}^2}{\Delta_2} t} + g_r \hat{\sigma}_{q_0}^- \hat{a}^\dagger + \text{h.c.}, \quad (\text{S6})$$

where $g_{\text{eff}}^{(j)} = g_p + g_{\text{qc}}^2/\Delta_j$. Finally, for perfectly symmetric devices $\Delta_1 = \Delta_2 = \Delta$, and, consequently, $g_{\text{eff}}^{(1)} = g_{\text{eff}}^{(2)} = g_{\text{eff}}$, it yields the effective Hamiltonian (with $\delta = g_{\text{qc}}^2/\Delta$)

$$\hat{H}_{\text{eff}} = \left(g_{\text{eff}} \hat{\sigma}_{q_1}^+ \hat{\sigma}_{q_0}^- + g_{\text{eff}} \hat{\sigma}_{q_2}^+ \hat{\sigma}_{q_0}^- + g_r \sigma_{q_0}^- \hat{a}^\dagger e^{-i\delta t} + \text{h.c.} \right). \quad (\text{S7})$$

When considering the Hamiltonian of Eq. (S7), we see that, due to the interaction of the dissipative cavity mode with the resetting head, the effective coupling between the erasing device and the working qubits allows the simultaneous reset for most of the states. However, a closer look will notice that the state $|\tilde{\Psi}_\phi\rangle = |\psi_\phi\rangle_{q_1 q_2} |0\rangle_{q_0 r}$, with $|\psi_\phi\rangle_{q_1 q_2} \propto |10\rangle_{q_1 q_2} + e^{i\phi} |01\rangle_{q_1 q_2}$ and $\phi \in [0, 2\pi]$, is a dark state for the previous Hamiltonian if $\phi = \pi$, because of the device's symmetry. To circumvent this issue, we resort to the tunability of the couplers' frequency.

Since Δ_1 and Δ_2 are functions of the ω_{c_1} and ω_{c_2} , respectively, they can be adjusted individually. Thus, by properly adjusting the frequency of the couplers, we can create different time dependencies on the Hamiltonian of Eq. (S6), and, hence, the state $|\tilde{\Psi}_\phi\rangle$ is no longer a dark state for $t > 0$. Additionally, for perfectly symmetric devices, by tuning the couplers' frequency, we change the effective coupling, which can make the dark state different from $|\tilde{\Psi}_\phi\rangle$. However, once the time dependency is always present for $\omega_{c_1} \neq \omega_{c_2}$, independently of the collective state in the beginning or during the dynamics, the time dependency of the Hamiltonian ensures the resetting.

For non-chiral devices, i.e., when we do not have perfectly symmetric devices, even though we have $g_{\text{eff}}^{(1)} \neq g_{\text{eff}}^{(2)}$ for the same Δ , different dark states can appear. However, once again, by exploring the tunable property of the couplers' frequencies, we can create well-known time dependencies that make the existing dark states vary in time and, consequently, be reset.

In the regime where the effective dynamics break down, i.e., when $|\Delta_n| \sim g_{\text{qc}}$, we must consider the full original Hamiltonian to explore the potential existence of dark states, paying particular attention to the interaction part \hat{H}_{qc} . By calculating the evolution of the state $|\Psi_\phi\rangle = |\psi_\phi\rangle_{q_1 q_2} |0\rangle_{q_0 c_1 c_2 r}$ through the expression $\hat{H} |\Psi_\phi\rangle$, it becomes clear that only the term $\hat{H}_{\text{qc}} |\Psi_\phi\rangle$ will be non-zero. In fact, this term gives

$$\begin{aligned} \hat{H}_{\text{qc}} |\Psi_\phi\rangle &= \frac{\hbar}{\sqrt{2}} \sum_{n=1}^2 \left[g_{\text{qc}} (\hat{\sigma}_{q_n}^+ + \hat{\sigma}_{q_0}^+) \hat{\sigma}_{c_n}^- + g_{\text{qc}} (\hat{\sigma}_{q_n}^- + \hat{\sigma}_{q_0}^-) \hat{\sigma}_{c_n}^+ + g_p \hat{\sigma}_{q_0}^+ \hat{\sigma}_{q_n}^- + g_p \hat{\sigma}_{q_0}^- \hat{\sigma}_{q_n}^+ \right] |10\rangle_{q_1 q_2} |0\rangle_{q_0 c_1 c_2 r} \\ &+ e^{i\phi} \frac{\hbar}{\sqrt{2}} \sum_{n=1}^2 \left[g_{\text{qc}} (\hat{\sigma}_{q_n}^+ + \hat{\sigma}_{q_0}^+) \hat{\sigma}_{c_n}^- + g_{\text{qc}} (\hat{\sigma}_{q_n}^- + \hat{\sigma}_{q_0}^-) \hat{\sigma}_{c_n}^+ + g_p \hat{\sigma}_{q_0}^+ \hat{\sigma}_{q_n}^- + g_p \hat{\sigma}_{q_0}^- \hat{\sigma}_{q_n}^+ \right] |01\rangle_{q_1 q_2} |0\rangle_{q_0 c_1 c_2 r} \\ &= \frac{\hbar}{\sqrt{2}} \left[g_{\text{qc}} |1\rangle_{c_1} |0\rangle_{q_1 q_2 q_0 c_2 r} + g_p |1\rangle_{q_0} |0\rangle_{q_1 q_2 c_1 c_2 r} \right] + e^{i\phi} \frac{\hbar}{\sqrt{2}} \left[g_{\text{qc}} |1\rangle_{c_2} |0\rangle_{q_0 c_1 q_1 q_2 r} + g_p |1\rangle_{q_0} |0\rangle_{q_1 q_2 c_1 c_2 r} \right] \\ &= \frac{\hbar g_{\text{qc}}}{\sqrt{2}} \left[|10\rangle_{c_1 c_2} + e^{i\phi} |01\rangle_{c_1 c_2} \right] |0\rangle_{q_1 q_2 q_0 r} + \frac{\hbar g_p}{\sqrt{2}} (1 + e^{i\phi}) |1\rangle_{q_0} |0\rangle_{q_1 q_2 c_1 c_2 r}. \end{aligned} \quad (\text{S8})$$

As previously noted in the effective dynamics, if $\phi = \pi$, the last term in Eq. (S8), which results from the interaction between the working qubits and the resetting head, vanishes. Consequently, the evolution of $|\Psi_{\phi=\pi}\rangle$ leads to a state proportional to $[|10\rangle_{c_1 c_2} - |01\rangle_{c_1 c_2}] |0\rangle_{q_1 q_2 q_0 r}$. This state, arising from the hopping terms in the interaction between the working qubits and their respective couplers, can be further evolved through a similar calculation, yielding

$$\hat{H}^2 |\Psi_{\phi=\pi}\rangle = \hat{H}_{\text{qc}}^2 |\Psi_{\phi=\pi}\rangle = \frac{\hbar^2 g_{\text{qc}}^2}{\sqrt{2}} \left[|10\rangle_{1 1_2} - |01\rangle_{q_1 q_2} \right] |0\rangle_{c_1 c_2 q_0 r} = \frac{\hbar^2 g_{\text{qc}}^2}{\sqrt{2}} |\Psi_{\phi=\pi}\rangle. \quad (\text{S9})$$

Therefore, if the initial state of the system is (or evolves into) $|\Psi_{\phi=\pi}\rangle$, the population remains trapped in the working qubits and couplers, leaving the resetting head unpopulated. As a result, the resetting process will not be achieved.

By analyzing Eqs. (S8) and (S9), it is not immediately clear that adjusting the frequencies of the couplers will result in satisfactory resetting because of the lack of them in the previous equations. However, this achievement is more readily observed through the effective dynamics, and it is corroborated by the results in the main text, where we simulate the dynamics for the state $|\Psi_{\phi=\pi}\rangle$ considering the full Hamiltonian and perform the resetting successfully.

This collective phenomenon may be observed in other models, such as those discussed in Refs. [29, 30], since they exhibit a similar configuration to the system studied here, which involves two systems coupled to a shared third system. Nevertheless, this discussion has not been addressed before within the context of the resetting process, likely because it is challenging to identify the specific states that exhibit these novel behaviors despite the concerns and the need to bypass them.

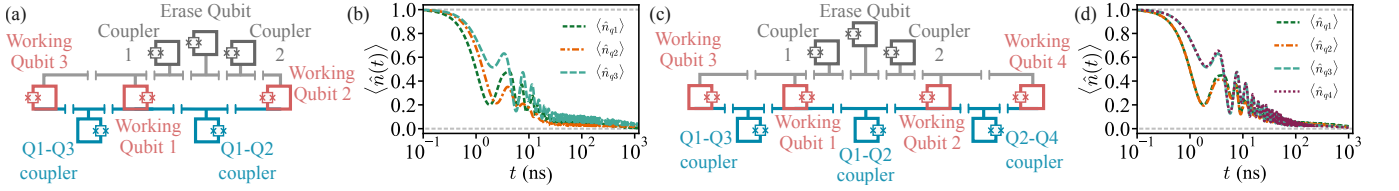


Figure S1. Panel (a) and (b) show three-qubit system considered for the simultaneous resetting and the populations for the three working qubits case, respectively. To this case, we assume $\omega_{c_1} = 3.1 \times 2\pi$ GHz and $\omega_{c_2} = \omega_{c_3} = 2.9 \times 2\pi$ GHz. Panel (c) and (d) show the four-qubit system and the populations in the qubits during the simultaneous resetting, respectively, where $\omega_{c_1} = \omega_{c_4} = 3.1 \times 2\pi$ GHz and $\omega_{c_2} = \omega_{c_3} = 2.9 \times 2\pi$ GHz. The other parameters for the device used here are $\omega_{q_i} = \omega_r = 3 \times 2\pi$ GHz, $g_q = 100 \times 2\pi$ MHz, $g_r = 120 \times 2\pi$ MHz, $g_{qc}^{(add)} = 90 \times 2\pi$ MHz, $g_p = 3 \times 2\pi$ MHz, and $\kappa = 150 \times 2\pi$ MHz.

Device's scalability

By utilizing the apparatus previously employed and considering the same resetting scheme components and configuration, additional working qubits can be incorporated into the model by coupling them to the existing qubits via couplers. Specifically, when considering the addition of one more working qubit, as depicted in Fig. S1a, the device Hamiltonian evolves to include the following terms

$$\hat{H}_0^{(add)} = \hbar\omega_{q_3}\hat{\sigma}_{q_3}^+\hat{\sigma}_{q_3}^- + \hbar\omega_{c_3}\hat{\sigma}_{c_3}^+\hat{\sigma}_{c_3}^-, \quad (S10a)$$

$$\hat{H}_{qc}^{(add)} = \hbar(g_{qc}^{(add)}(\hat{\sigma}_{q_1}^+ + \hat{\sigma}_{q_3}^+)\hat{\sigma}_{c_3}^- + g_p\hat{\sigma}_{q_1}^+\hat{\sigma}_{q_3}^- + \text{h.c.}), \quad (S10b)$$

with $\hat{H}_0^{(add)}$ describing the free energies of the new components, where, following the model of Fig. S1a, q_3 represents the working qubit 3 and c_3 represents the coupler Q1-Q3. Still, the Hamiltonian $\hat{H}_{qc}^{(add)}$ describes the interactions between the additional qubit and coupler, as well as the qubit-qubit interaction. Extending this framework to four working qubits, i.e., by adding two more qubits, as shown in Fig. S1c, the extra Hamiltonians are

$$\hat{H}_0^{(add)} = \hbar(\omega_{q_4}\hat{\sigma}_{q_4}^+\hat{\sigma}_{q_4}^- + \omega_{q_3}\hat{\sigma}_{q_3}^+\hat{\sigma}_{q_3}^- + \omega_{c_4}\hat{\sigma}_{c_4}^+\hat{\sigma}_{c_4}^- + \omega_{c_3}\hat{\sigma}_{c_3}^+\hat{\sigma}_{c_3}^-); \quad (S11a)$$

$$\hat{H}_{qc}^{(add)} = \hbar(g_{qc}^{(add)}((\hat{\sigma}_{q_1}^+ + \hat{\sigma}_{q_3}^+)\hat{\sigma}_{c_3}^- + (\hat{\sigma}_{q_2}^+ + \hat{\sigma}_{q_4}^+)\hat{\sigma}_{c_4}^-) + g_p(\hat{\sigma}_{q_1}^+\hat{\sigma}_{q_3}^- + \hat{\sigma}_{q_2}^+\hat{\sigma}_{q_4}^-) + \text{h.c.}), \quad (S11b)$$

where, following the model of Fig. S1c, q_4 represents the working qubit 4 and c_4 represents the coupler Q2-Q4.

By simulating the full dynamics described by the Schrödinger equation, we are able to reset the three and four qubits simultaneously, Figs. S1b and S1d, respectively. As shown in Fig. S1, in both cases, the resetting times are characterized by $\tau_{\text{res}} \sim 1 \mu\text{s}$. Even if parameter optimization can reduce the overall resetting time, these values remain comparable to the natural decay time of the working qubits. Consequently, with the current state-of-the-art superconducting qubits, incorporating five or more working qubits is not advantageous, considering the time spent during the resetting task. However, it can be more feasible shortly with the advancement of the platform and the enhancement of the qubits' lifetime.

Moreover, unlike the scheme considered in the main text, the resetting process is no longer fully controllable in these expanded configurations since we cannot reset each qubit individually. For instance, in the case of three qubits, resetting qubit q_3 necessitates the simultaneous resetting of qubit q_1 . Similarly, in the four-qubit case, qubit q_2 will be reset whenever the information stored in qubit q_4 is erased. This limitation reduces both the device's control and adaptability.